

Heteromolecular grids of free-base and zinc-tetra(4-pyridyl)porphyrins with benzenetetracarboxylic acid

Rajesh Koner · Israel Goldberg

Received: 16 April 2009 / Accepted: 15 June 2009 / Published online: 9 July 2009
© Springer Science+Business Media B.V. 2009

Abstract This study describes the formation of heteromolecular networks involving the 1,2,4,5-benzenetetracarboxylic acid (BTCA) and either the free-base or zinc-metallated tetra(4-pyridyl)porphyrin (TPyP or Zn-TPyP, respectively), taking advantage of the complementary tetradentate H-atom donor and H-atom acceptor capacity of the component species. The reaction of BTCA with TPyP yields flat square-grid-type hydrogen bonded arrays, wherein every BTCA moiety interacts with four different porphyrin units and each one of the latter links laterally to four different tetraacid molecules. Replacement of TPyP by Zn-TPyP adds axial coordination capacity to the porphyrin unit and changes the intermolecular interaction pattern. In this case, the supramolecular self-assembly involves *trans*-axial coordination of BTCA to Zn-TPyP, into a 2:1 complex of the two species, as well as extended hydrogen bonding in four lateral directions between the (BTCA)₂(Zn-TPyP) units thus formed. The hydrogen-bond networking takes place between the four *N*(pyridyl)-sites of the porphyrin scaffold and the axial tetracid ligands of four neighboring complexes. In the two crystals, the open hydrogen bonded molecular networks stack in an offset manner, incorporating molecules of the 1,1,2,2-tetrachloroethane solvent within channel zones that penetrate through the layered structure. Application of the TPyP scaffold in the formation of hydrogen-bonded (rather than coordination-driven) assemblies has not been explored prior to our work on this subject.

Keywords Tetra(4-pyridyl)porphyrin · Molecular networks · Hydrogen bonding

Introduction

The 5,10,15,20-tetra(4-pyridyl)porphyrin moiety (TPyP) has a planar and rigid structure, bearing laterally diverging pyridyl functions prone to interact with complementary neighboring entities through coordination or hydrogen bonding. Free-base TPyP and its core-metallated analogs (M-TPyP) are readily available [1, 2]. The Zn-TPyP complex was successfully used already nearly 20 years ago for the assembly of self-coordinated oligomeric or 1-D polymeric arrays [3]. This pioneering study by Fleischer et al. was soon followed by two other landmark publications of TPyP-based coordination polymers of single-framework three-dimensional solids. In appropriate conditions the Zn-TPyP self-assembles into a robust honeycomb architecture (with trigonal R-3 space group symmetry), perforated by 0.5–0.6 nm wide channels, and exhibits an unprecedented high thermal stability to >400 °C [4]. Isomorphous structures were achieved at a later date with the Co-TPyP and Mn-TPyP scaffolds [5], as well as with related 5,15-dipyridyl-10,20-diphenyl/di(4-iodophenyl) porphyrin scaffolds [6, 7]. Materials of this structure-type represent genuine porous solids, revealing remarkable sorption and desorption features. Another approach was to take advantage of the coordination ability of the peripheral pyridyl sites to crosslink the TPyP units with the aid of exocyclic metal linkers. The seminal work of Robson et al. along this line of reasoning demonstrated the formulation of a 3D coordination framework containing large inter-porphyrin voids of nano-metric (≥ 1 nm) dimensions by reacting Cu(II)-TPyP with Cu(I) connectors (accompanied by suitable counter

R. Koner · I. Goldberg (✉)
School of Chemistry, Sackler Faculty of Exact Sciences,
Tel Aviv University, Ramat Aviv, 69978 Tel Aviv, Israel
e-mail: goldberg@post.tau.ac.il

ions) that bridged between the pyridyl sites of neighboring molecules [8]. This framework collapsed, however, on removal of the lattice-trapped solvent, not being able to sustain the large void space in the condensed solid phase. The above observations stimulated in subsequent years an extensive research on coordination polymerization of the TPyP and M–TPyP ligands through diverse metal ion connectors [9–13]. With the free base porphyrin, and in order to prevent the competing metalation of the tetraaza porphyrin core, the use of relatively large transition metals was required to this end [10]. Various modes of direct self-assembly of the M–TPyP scaffold, without resorting to exocyclic metal bridges, have also been reported [4–7, 14, 15]. Coordination polymers of BTCA with metal ions are known as well [16, 17].

In contrast to the so intensive investigations of the (M)–TPyP system in the coordination-driven self-assembly context over the last two decades, the hydrogen-bonding capacity of this scaffold in the formulation of supramolecular networks has not been explored. This can be attributed to the considerably higher robustness of coordination-based framework solids in relation to materials sustained by thermodynamically labile hydrogen bonding. More recently, however, surface crystallization of supramolecular systems is gaining increasing attention, and intermolecular ordering via hydrogen bonding synthons appears highly significant as well [18–20]. Here we report on the first crystallographic characterization of targeted hetero-molecular networks involving the TPyP/Zn–TPyP and BTCA moieties, and the channel-type clathrates they form with 1,1,2,2-tetrachloroethane (TCE): (TPyP)·(BTCA)·(TCE)₄ (**1**) and (Zn–TPyP)·(BTCA)₂·(TCE)₄ (**2**).

Experimental section

Synthetic and crystallization procedures

All reagents and solvents were purchased from commercial sources and used without further purification. Crystals of compounds **1** and **2** were prepared using the layering technique at room temperature. The FT-IR spectra were recorded in the range of 400–4,000 cm⁻¹ from KBr pellets (Aldrich 99%+, FT-IR grade), using a BRUKER PS15 spectrophotometer. Compound **1** was obtained by layering a dilute DMF solution of BTCA (7.87 × 10⁻³ M, 4 mL) over a dilute solution of TPyP, in a 3:1 solubilizing mixture of TCE and methanol (~1.6 × 10⁻³ M, 10 mL). The reaction mixture was left at room temperature for several days to yield deep-red crystals of **1**. The crystals were washed with the solvent mixture, and dried in air. IR (KBr/cm⁻¹): 1,717 m (ν_{COOH}); 1,595 s, 1,427 m, 1,142 w, 1,095 m, 969 m, 798 s. For compound **2**: First, 10 mL of a

1.47 × 10⁻³ M solution of Zn–TPyP, in a mixture of TCE and methanol was placed at the bottom of a glass tube. Next, 2 mL of pure methanol was carefully layered on top of it. Finally a 4 mL layer of a 7.87 × 10⁻³ M methanol solution of BTCA was layered on top. The solutions were left to diffuse into one another through the buffering methanol zone at room temperature. Deep red crystals appeared after a few days, were collected by filtration, washed with TCE and dried in air. 1,718 m (ν_{COOH}); 1,625 s, 1,598 m, 1,519 m, 1,506 m, 1,481 w, 1,202 m, 1,171 m, 1,000 s, 990 s, 752 s, 720 m. The FT-IR spectra of the two compounds exhibit a medium intensity broad band within 2,200–2,800 cm⁻¹, which is attributed to the O–H stretching vibration of a strongly hydrogen-bonded carboxylic acid group; in addition, lack of medium/strong intensity bands in the IR region of 1,300–1,420 cm⁻¹ (characteristic to the symmetric COO⁻ stretch) confirms that no deprotonation of the carboxylic acid groups has occurred in either case [21]. The uniformity of the crystalline solids **1** and **2** was confirmed in each case by repeated measurements of the unit-cell dimensions from several randomly chosen crystals.

Crystal structure determinations

The X-ray measurements (Nonius KappaCCD diffractometer, MoKα radiation) were carried out at 110(2) K. The structures were solved by direct methods (SIR-97) and refined by full-matrix least-squares (SHELXL-97). All non-hydrogen atoms were refined anisotropically. The hydrogen atoms were either located in idealized/calculated positions or in difference-Fourier maps. They were refined using a riding model, with U_{iso} = 1.2 U_{eq} of the parent atom.

Crystal Data: **1**, [(C₄₀H₂₆N₈)(C₁₀H₆O₈)·4(C₂H₂Cl₄)]: formula weight 1544.18, triclinic, space group *P*-1, *a* = 6.6083(3), *b* = 15.6335(4), *c* = 17.2037(6) Å, α = 112.143(1), β = 100.640(1), γ = 97.413(1)°, *V* = 1578.96(10) Å³, *Z* = 1, *T* = 110(2) K, *D*_{calc} = 1.624 g cm⁻³, μ(MoKα) = 0.76 mm⁻¹, 29,409 collected data and 7,466 unique reflections (θ_{max} = 27.86°), *R*_{int} = 0.034. The final *R*₁ = 0.063 for 6,097 observations with *F*_o > 4σ(*F*_o), *R*₁ = 0.074 (*wR*₂ = 0.193) for all unique data, 363 refined parameters, |Δρ| ≤ 0.84 e/Å³. CCDC 726894. **2**, [(C₄₀H₂₄N₈Zn)·2(C₁₀H₆O₈)·4(C₂H₂Cl₄)]: formula weight 1861.68, triclinic, space group *P*-1, *a* = 11.5366(2), *b* = 12.6817(2), *c* = 12.9893(3) Å, α = 81.4271(8), β = 87.8912(7), γ = 78.0338(6)°, *V* = 1838.28(6) Å³, *Z* = 1, *T* = 110(2) K, *D*_{calc} = 1.682 g cm⁻³, μ(MoKα) = 0.99 mm⁻¹, 33,869 collected data and 8,702 unique reflections (θ_{max} = 27.84°), *R*_{int} = 0.047. The final *R*₁ = 0.067 for 6,311 observations with *F*_o > 4σ(*F*_o), *R*₁ = 0.085 (*wR*₂ = 0.171) for all unique data, 454 refined

parameters, $|\Delta\rho| \leq 0.65 \text{ e}/\text{\AA}^3$. CCDC 726895. In the two structures molecules of the TPyP, Zn–TPyP and BTCA units are located on centers of inversion. The TCE solvent, which is accommodated in intralattice voids, tends to reveal conformational as well as rotational disorder. Two out of four solvent molecules (per unit-cell) in **1** and the four solvent species in **2**, although clearly identified in electron density maps, could not be precisely modelled by discrete atoms due to such disorder. Their contributions were subtracted from the corresponding diffraction patterns by the “Squeeze” method [22], and excluded from the final refinement calculations. The voids accessible to the excluded solvents and the residual electron density in them were assessed to be 313 \AA^3 and 114 e per unit-cell in **1** and 686 \AA^3 and 256 e per unit-cell in **2** (more accurate assessments of the solvent content by thermogravimetric analyses could not be performed due to the microgram scale of the preparative experiments). Irrespectively, the crystallographic evaluations provided reliable structural models of the porphyrin-BTCA molecular networks in the two solids.

Results and discussion

The TPyP and BTCA components provide excellent building blocks for the construction of hetero-molecular networks sustained by cooperative hydrogen bonding. Both have an aromatic framework which bears four laterally extending functions, the 4-pyridyl substituents in TPyP acting as H-atom acceptors, and the four carboxylic acid residues in BTCA as complementary proton donors. Full utilization of the $\text{COOH}\cdots\text{N}(\text{pyridyl})$ H-bonding capacity in **1**, facilitated with rotational degree of freedom of the carboxylic groups, leads to the formation of an open square-grid-type network. In the latter, every TPyP unit is linked to four adjacent molecules of BTCA and every tetraacid is connected to four different porphyrins, hence the 1:1 ratio of the interacting components. The relatively short hydrogen bonding distances $\text{O}\cdots\text{N} = 2.579(2)$ and $2.598(3) \text{ \AA}$ reflect on a strong interaction [23]. The assembly of the open grid is templated by the TCE solvent, as depicted in Fig. 1. Molecules of TCE occupy the intermolecular voids, either in an ordered (which is associated with the formation of weak $\text{C}-\text{H}_{\text{TCE}}\cdots\text{O}_{\text{BTCA}}$) or a disordered manner, and stabilize the networked structure.

In the crystal the TPyP and BTCA molecules are located on centers of inversion. The hydrogen-bonded layers are essentially planar, being inclined by about 60° with respect to the $(0,1,1)$ plane of the crystal. The porphyrin molecules tightly offset stack along the $(x, 1/2, 1/2)$ axis with an interplanar distance of 3.5 \AA , and the similarly separated BTCA units along the $(x, 0, 0)$ direction. The solvent moieties aggregate in channel type voids propagating along

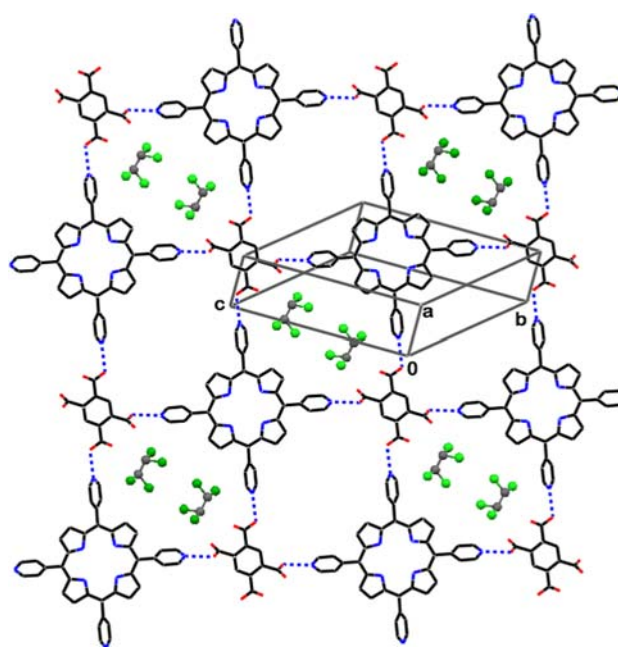


Fig. 1 Illustration of the 1:1 hydrogen bonded (dashed lines) assembly of TPyP with BTCA, into a square-grid network, in **1**. Molecules of TCE are accommodated in pairs within the interporphyrin voids, ordered (around inversion centre at $0,0,1/2$, shown in ball-and-stick representation) and disordered (around inversion at $0,1/2,0$, omitted) solvent occupying alternating sites. The H-atoms are omitted

the $(x, 1/2, 0)$ and $(x, 0, 1/2)$ axes, through the bi-component hydrogen-bonded networks, imparting to **1** a channel-clathrate architecture. An edge-on view of the network assemblies that cross the eight corners of the unit-cell is shown in Fig. 2.

The additional axial coordination capacity of the ZnTPyP scaffold modifies significantly the supramolecular aggregation in **2**. It is known that ZnTPyP reveals predominantly five-coordinate environment associating with a single axial ligand, yet its four- and six-coordinate (with two axial ligands) forms have also been reported [4, 7, 24]. Its reaction with BTCA in the present case results in the formation of six-coordinate $(\text{ZnTPyP})(\text{BTCA})_2$ complexes. The axial ligation on both sides is characterized by relatively long $\text{Zn}-\text{O}_{\text{BTCA}}$ distances (typical to a six-coordinate zinc complex) of $2.492(3) \text{ \AA}$ [4, 25]. The mean planes of the BTCA units are roughly parallel to the porphyrin macrocycle. Due to the 1:2 stoichiometry of the repeating unit, the ratio between the number of the available proton acceptor (in ZnTPyP) and proton donor (in the two BTCA's) sites is also 1:2. As a result, the excessive number of the latter is utilized in intramolecular hydrogen bonding within the tetraacid species, the two bonds formed between two pairs of neighboring carboxylic acid groups are at $\text{O}\cdots\text{O} = 2.298(4)$ and $2.436(4) \text{ \AA}$. The remaining two O–H proton donors on each of the axial BTCA ligands are then

Fig. 2 An edge-on view of the hydrogen bonded networks that pass through the eight corners of the unit-cell in **1**. The TCA solvent is excluded

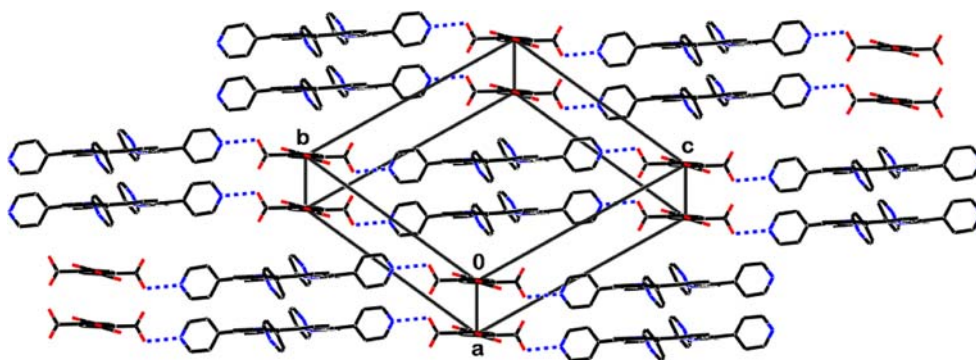
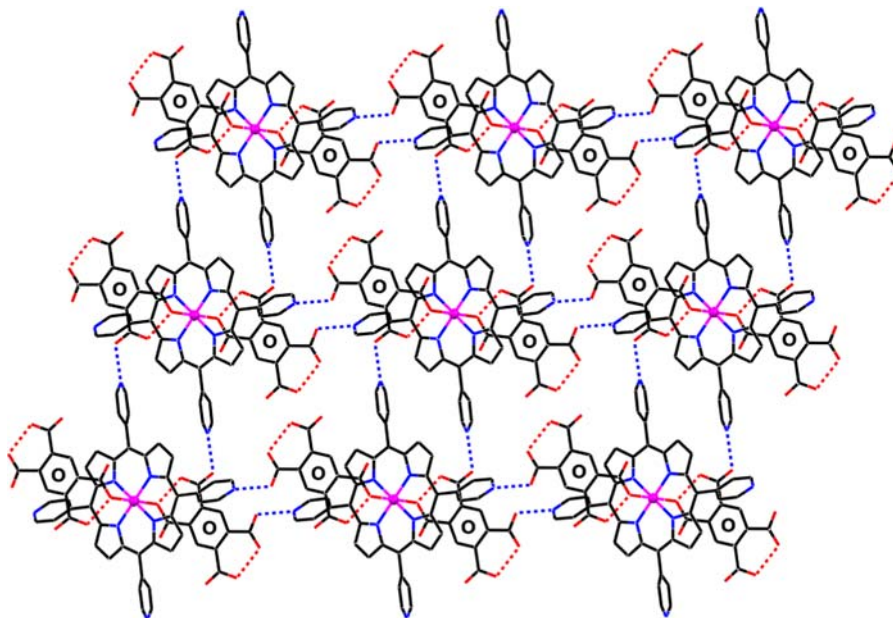


Fig. 3 The layered supramolecular open-grid aggregation in **2**. The intra- and inter-molecular hydrogen bonds are depicted by *dashed lines*. The Zn-ions are shown as *small spheres*, and the benzene rings of BTCA are marked by *circles*. The solvent species and the H-atoms are omitted



used in *intermolecular* associations. The supramolecular aggregation via hydrogen bonds takes place now between the $(\text{ZnTPyP})(\text{BTCA})_2$ entities, as shown in Fig. 3.

The combined coordination and hydrogen bonding creates three-molecule thick network. The porphyrin constituent of one complex binds laterally to the axial ligands of four neighboring complexes through its four pyridyl sites. In addition, each of the two BTCA components forms two additional hydrogen bonds to the surrounding porphyrins at O...N distances of 2.570(3) and 2.586(3) Å. Thus, every unit of the 1:2 complex is engaged in total of eight nearly linear hydrogen bonds to its neighbors, yielding an open 2D grid. In order to facilitate this binding pattern (and allow efficient association of the lateral pyridyl groups with the axial ligands on the upper and lower sides of neighboring entities) the porphyrin macrocycle is inclined by about 15° with respect to the mean plane of the hydrogen bonded network. The two-dimensional network assemblies stack in the crystal along the $[1, 0, -1]$ axis. At the interface between consecutive layers, effective π - π interactions operate between the axial BTCA ligands from the lower

side of one layer and the upper side of an adjacent layer (Fig. 4). The distance between the overlapping benzene cores of the corresponding BTCA molecules is 3.315 Å.

Structure **2** represents also a channel clathrate. View of the structure down the *c*-axis reveals wide solvent-accessible channels (Fig. 5), which propagate through the layered networks and enclathrate the severely disordered molecules of the tetrachloroethane solvent (four molecules per unit cell). The distances between the zinc centers of the complexes that encircle the channels are 11.54 and 12.68 Å, the corresponding van der Waals cross-sectional dimensions of the solvent-accessible voids centered around inversion at $\frac{1}{2}, \frac{1}{2}, \frac{1}{2}$ being approximately 5.5×7.0 Å.

In both structures the TCE solvent serves also as a template (alternatively, 1,2-dichlorobenzene can be used to this end) around which the network arrays self assemble and crystallize out from the given reaction mixture. Enclathration of the solvent in the crystal lattice along with the porphyrin and BTCA components reduces the desolvation energy lost during the crystallization reactions. The resulting chltrates are stable for days when kept in a closed vial at

Fig. 4 Projection of structure **2** down the *b*-axis of the unit-cell, showing edge-on three consecutive supramolecular layers. Note the π - π stacking of the BTCA ligands of adjacent layers, and the inclination of the porphyrin units with respect to the hydrogen-bonded layers. The intermolecular hydrogen bonds are depicted by *dashed lines*. The Zn-ions are shown as *small spheres*. The solvent species and the H-atoms are omitted

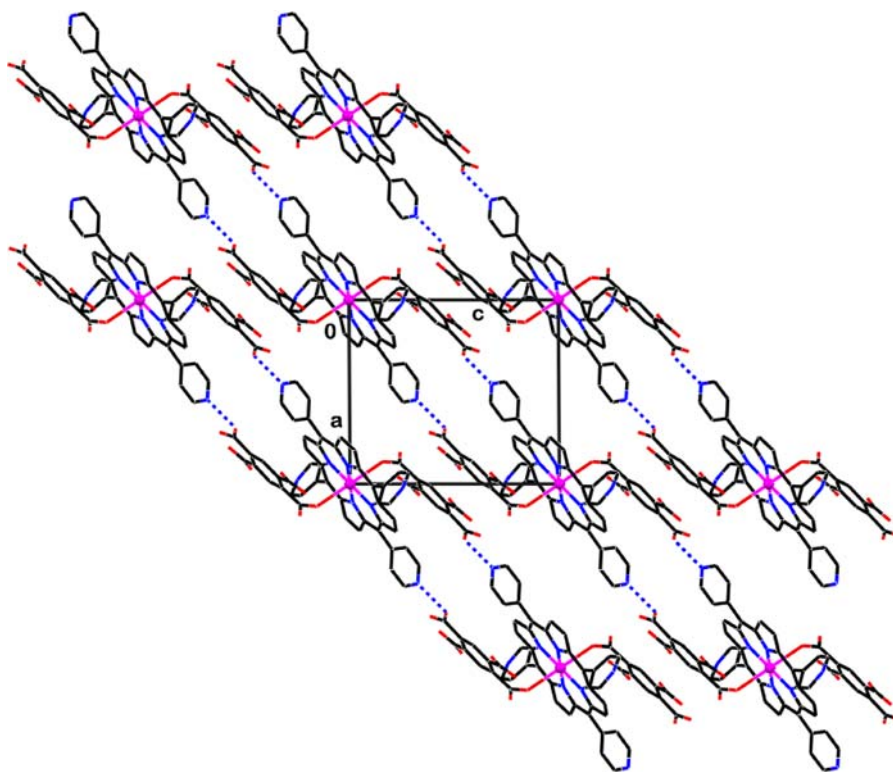
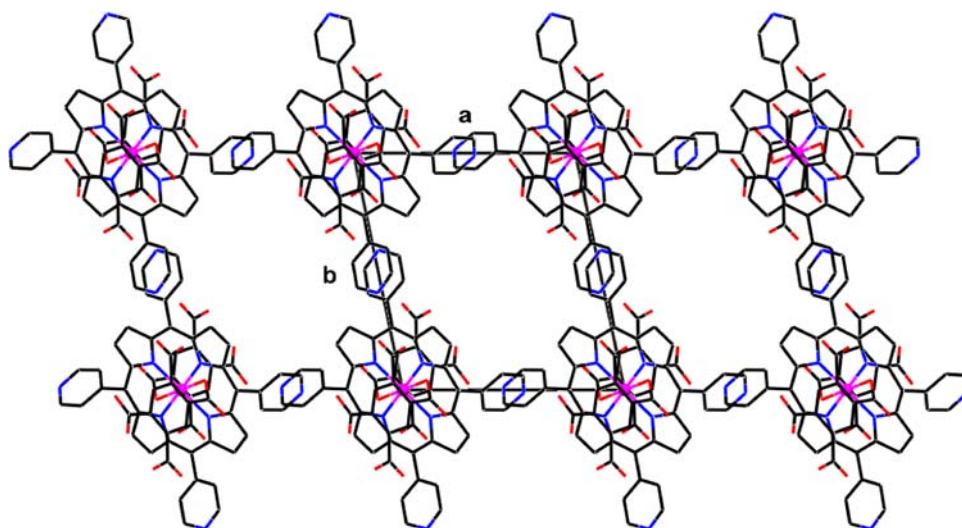


Fig. 5 The clathrate nature of **2**. Projection of the crystal structure down the *c*-axis, showing the sizeable channel voids centred around inversion at $\frac{1}{2}, \frac{1}{2}, \frac{1}{2}$ that accommodate the disordered TCE solvent (not shown)



ambient temperature. Although the enthalpies of the hydrogen bonds and π - π stacking forces when considered alone are relatively small [23, 26], their cooperative effect approaches the strength of a covalent bond, and in the presence of suitable templates it appears to be adequate to stabilize the observed channeled-layered architectures. The space required to accommodate four molecules of TCE per unit-cell in the two structures is relatively large, amounting in each case to nearly 40% of the total crystal volume. Not surprisingly, therefore upon removal of the templating

solvent, the crystalline network solids deteriorate into amorphous materials.

Conclusion

The utility of the TPyP scaffold as an effective building block for the construction of molecular networks sustained primarily by hydrogen bonds via complementary organic ligands has been demonstrated here for the first time. As

the square-planar TPYP framework may function through its lateral pyridyl groups as tetradentate proton acceptor, application of tetradentate proton donors of similarly square-planar geometry was anticipated to be most suitable to this end. The strong $\text{COOH}\cdots\text{N}_{\text{pyridyl}}$ synthon [23], combined with cooperative hydrogen bonding interactions in four different directions and the use of favourable reaction environment and templating solvent led to a successful design of heteromolecular networks with the TPYP/ZnTPYP and BTCA reagents. Similar modes of networking sustained by hydrogen bonding of the tetra(4-carboxyphenyl)porphyrin scaffold have been reported [27, 28]. The current findings are of further significance to studies of surface-based crystallizations of hydrogen bonded monolayer and multilayer networks on various substrates [18–20], associated with the design of novel molecular devices. Further structural characterizations of TPYP-based hydrogen-bonded 2D molecular networks with related tri- and tetra-carboxylic ligands are timely to this end.

Acknowledgment This research was supported by The Israel Science Foundation (grant No. 502/08).

References

- Fleischer, E.B.: α , β , γ , δ -Tetra-(4-pyridyl)-porphine and some of its metal complexes. *Inorg. Chem.* **1**, 493–495 (1962)
- Collins, D.M., Hoard, J.L.: The crystal structure and molecular stereochemistry of α , β , γ , δ -tetra(4-pyridyl)-porphinatemonopyridinezinc(II). Appraisal of bond strain in the porphine skeleton. *J. Am. Chem. Soc.* **92**, 3761–3771 (1970)
- Fleischer, E.B., Shachter, A.M.: Coordination oligomers and a coordination polymer of zinc tetraarylporphyrins. *Inorg. Chem.* **30**, 3763–3769 (1991)
- Krupitsky, H., Stein, Z., Goldberg, I., Strouse, C.E.: Crystalline complexes, coordination polymers and aggregation modes of tetra(4-pyridyl)porphyrin. *J. Incl. Phenom. Mol. Recognit. Chem.* **18**, 177–192 (1994)
- Lin, K.-J.: SMTP-1: the first functionalized metalloporphyrin molecular sieves with large channels. *Angew. Chem. Int. Ed. Engl.* **38**, 2730–2732 (1999)
- Dieters, E., Bulach, V., Hossein, M.W.: Reversible single-crystal-to-single-crystal guest exchange in a 3-D coordination network based on a zinc porphyrin. *Chem. Commun.* 3906–3908 (2005)
- Lipstman, S., Muniappan, S., Goldberg, I.: Supramolecular reactivity of porphyrins with mixed iodophenyl and pyridyl *meso*-substituents. *Cryst. Growth Des.* **8**, 1682–1688 (2008)
- Abrahams, B.F., Hoskins, B.F., Michail, D.M., Robson, R.: Assembly of porphyrin building-blocks into network structures with large channels. *Nature* **369**, 727–729 (1994)
- Hagman, D., Hagman, P.J., Jubieta, J.: Solid-state coordination chemistry: the self-assembly of microporous organic-inorganic hybrid frameworks constructed from tetrapyrrolylporphyrin and bimetallic oxide chains or oxide clusters. *Angew. Chem. Int. Ed. Engl.* **38**, 3165–3168 (1999)
- Sharma, C.V.K., Broker, G.A., Huddleston, J.G., Baldwin, J.W., Metzger, R.M., Rogers, R.D.: Design strategies for solid-state supramolecular arrays containing both mixed-metalated and freebase porphyrins. *J. Am. Chem. Soc.* **121**, 1137–1144 (1999)
- Pan, L., Kelly, S., Huang, X., Li, J.: Unique 2D metalloporphyrin networks constructed from iron(II) and *meso*-tetra(4-pyridyl)porphyrin. *Chem. Commun.* 2334–2335 (2002)
- Carlucci, L., Ciani, G., Proserpio, D.M., Porta, F.: Open network architectures from the self-assembly of AgNO_3 and 5,10,15,20-tetra(4-pyridyl)porphyrin building blocks: the exceptional self-penetrating topology of the 3D network of $[\text{Ag}_8(\text{Zn}^{\text{II}}\text{TPYP})_7(\text{H}_2\text{O})_2](\text{NO}_3)_8$. *Angew. Chem. Int. Ed. Engl.* **42**, 317–322 (2003)
- Ohmura, T., Usuki, A., Fukumori, K., Ohta, T., Tatsumi, K.: New porphyrin-based metal-organic framework with high porosity: 2-D infinite 22.2-Å square-grid coordination network. *Inorg. Chem.* **45**, 7988–7990 (2006)
- Diskin-Posner, Y., Patra, G.K., Goldberg, I.: Supramolecular assembly of metalloporphyrins in crystals by axial coordination through amine ligands. *Dalton Trans.* 2775–2782 (2001)
- Ring, D.J., Aragoni, M.C., Champness, N.R., Wilson, C.: A coordination polymer supramolecular isomer formed from a single building block: an unexpected porphyrin ribbon constructed from zinc(tetra(4-pyridyl)porphyrin). *CrystEngComm* **7**, 621–623 (2005)
- Fabelo, O., Cañadillas-Delgado, L., Pasán, J., Ruiz-Pérez, C., Julve, M.: Influence of the presence of divalent first-row transition metal ions on the structure of sodium(I) salts of 1,2,3,4-benzenetetracarboxylic acid (H_4BTA). *CrystEngComm* **8**, 338–345 (2006)
- Ghosh, S.K., Bharadwaj, P.K.: Puckered-boat conformation hexameric water clusters stabilized in a 2D metal-organic framework structure built from Cu(II) and 1,2,4,5-benzenetetracarboxylic acid. *Inorg. Chem.* **43**, 5180–5182 (2004)
- Shi, N., Yin, G., Han, M., Jiang, L., Xu, Z.: Self-assembly of two different hierarchical nanostructures on either side of an organic supramolecular film in one step. *Chemistry* **14**, 6255–6259 (2008)
- Blunt, M., Lin, X., Gimenez-Lopez, M.C., Schröder, M., Champness, N.R., Beton, P.H.: Directing two-dimensional molecular crystallization using guest templates. *Chem. Commun.* 2304–2306 (2008)
- Zhou, H., Dang, H., Yi, J.-H., Nanci, A., Rocherfort, A., Wuest, J.D.: Frustrated 2D molecular crystallization. *J. Am. Chem. Soc.* **129**, 13774–13775 (2000)
- Johnson, S.L., Rumon, K.A.: Infrared spectra of solid 1:1 pyridine-benzoic acid complexes; the nature of the hydrogen bond as a function of the acid-base levels in the complex. *J. Phys. Chem.* **69**, 74–86 (1965)
- Spek, A.L.: Single-crystal structure validation with the program *PLATON*. *J. Appl. Crystallogr.* **36**, 7–13 (2003)
- Gilli, P., Pretto, L., Bertolasi, V., Gilli, G.: Predicting hydrogen-bond strengths from acid-base molecular properties. The pK_a slide rule: toward the solution of a long-lasting problem. *Acc. Chem. Res.* **42**, 33–44 (2009)
- Goldberg, I.: Crystal engineering of porphyrin framework solids. *Chem. Commun.* 1243–1254 (2005)
- Allen, F.H.: The Cambridge crystallographic database: a quarter of a million crystal structures and rising. *Acta Crystallogr. B* **58**, 380–388 (2002)
- Jeffrey, G.A.: *An Introduction to Hydrogen Bonding*. Oxford University Press, Oxford (1997)
- Diskin-Posner, Y., Goldberg, I.: From porphyrin sponges to porphyrin sieves: a unique crystalline lattice of aquazinc tetra(4-carboxyphenyl)porphyrin with nanosized channels. *Chem. Commun.* 1961–1962 (1999)
- Vinodu, M., Goldberg, I.: Complexes of hexamethylenetetramine with zinc-tetraaryl-porphyrins, and their assembly modes in crystals as clathrates and hydrogen-bonding network polymers. *New J. Chem.* **28**, 1250–1254 (2004)